J Assist Reprod Genet (2016) 33:929–938
DOI 10.1007/s10815-016-0716-2

GAMETE BIOLOGY

Dynamic changes in mitochondrial distribution in human oocytes during meiotic maturation

Yuki Takahashi[1] · Shu Hashimoto[1] · Takayuki Yamochi[1] · Hiroya Goto[1] · Masaya Yamanaka[1] · Ami Amo[1] · Hiroshi Matsumoto[1] · Masayasu Inoue[1] · Keijiro Ito[1] · Yoshiharu Nakaoka[1] · Nao Suzuki[2] · Yoshiharu Morimoto[1]

Received: 16 December 2015 / Accepted: 11 April 2016 / Published online: 27 April 2016

Abstract
Purpose The change of mitochondrial distribution in human oocytes during meiotic maturation was assessed using 223 human oocytes donated from patients undergoing fertility treatment between June 2013 and February 2016.
Methods Live cell images of fluorescence-labelled mitochondria in human oocytes were analysed to investigate dynamic changes in mitochondrial distribution during meiotic maturation using a confocal microscope combined with an incubator in the presence or absence of colchicine and cytochalasin B, inhibitors for tubulin and actin filament, respectively. Subcellular distribution of mitochondria in human oocytes was also assessed at various stages using a transmission electron microscope (TEM).
Results Live cell imaging analysis revealed that the mitochondria-occupied cytoplasmic area decreased from 83 to 77 % of the total cytoplasmic area around 6 h before germinal vesicle breakdown (GVBD) and that mitochondria accumulated preferentially close to the perinuclear region. Then, the mitochondria-distributed area rapidly increased to 85 % of total cytoplasm at the time of GVBD. On the other hand, there was no significant change in mitochondrial distribution before and after polar body extrusion. Such changes in mitochondrial localization were affected differently by colchicine and cytochalasin B. Most of mitochondria in the cytoplasm formed cluster-like aggregates before GVBD while they distributed homogeneously after GVBD.
Conclusions Most mitochondria localized predominantly in the non-cortical region of the cytoplasm of GV stage-oocytes, while the mitochondria-occupied area decreased transiently before GVBD and increased rapidly to occupy the entire area of the cytoplasm at GVBD by some cytoskeleton-dependent mechanism.

Keywords Cytoskeleton · Human oocyte maturation · Mitochondrial dynamics

Capsule The mitochondria-occupied area decreased transiently before GVBD and increased rapidly to occupy the entire area of the cytoplasm at GVBD by some cytoskeleton-dependent mechanism.

✉ Shu Hashimoto
hashimoto@ivfnamba.com

[1] IVF Namba Clinic, 1-17-28 Minamihorie, Nishi-ku, Osaka 550-0015, Japan

[2] Department of Obstetrics and Gynecology, St. Marianna University School of Medicine, Kanagawa, Japan

Introduction

Maturation of mammalian oocytes involves distinct events in the nucleus and the cytoplasm [1, 2]. Although nuclear maturation that involves germinal vesicle breakdown (GVBD), chromosomal condensation and alignment, anastral spindle formation and polar body extrusion has been studied extensively, cytoplasmic maturation is less understood.

Mitochondria-generated ATP plays important roles in both nuclear and cytoplasmic maturation of oocytes [3–8]. Mitochondria change their distribution in the cytoplasm during the maturation of oocytes in human [1, 2, 7] and mice [9–11]. Several studies suggested that the subcellular distribution of mitochondria is one of the important factors for oocyte maturation and embryo development [11–20]. Mitochondria in murine oocytes have been shown to form aggregates around the GV, disperse throughout the cytoplasm at G2/M transition, and then distribute across the cytoplasm of oocytes at the time of polar body extrusion [21, 22]. In contrast, mitochondria in the cytoplasm of porcine oocytes took on an entirely different aspect showing

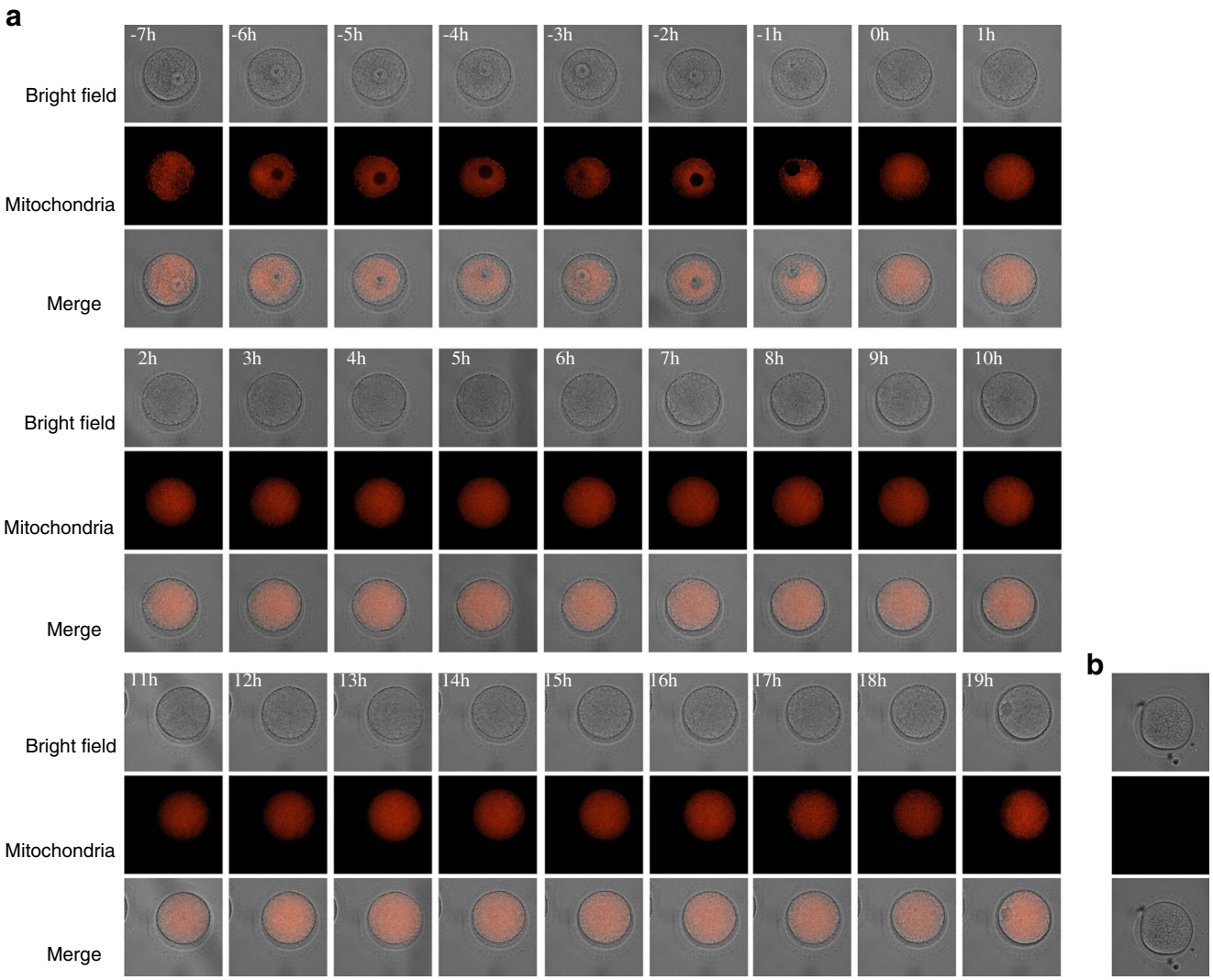

Fig. 1 Live cell imaging of mitochondrial dynamics during meiotic maturation of human oocytes. *Images of first, second and third rows* show bright field, mitochondria and merged images. *Numbers on the upper left corner in each panel* show elapsed times (in hour) before or after GVBD (**a**). Non-labelled oocytes (**b**)

homogeneous localization and movement towards the central area of cells after GVBD [15]. Moreover, no marked change in the mitochondrial distribution was observed during bovine oocyte maturation [6]. Thus, the subcellular distribution of mitochondria during oocyte maturation seems to differ from one species to another. Reports of mitochondrial behaviour in human oocytes are conflicting. Wilding et al. [16] reported that mitochondria did not change in their distribution during oocyte maturation, while Liu et al. [23] showed that they spread from the juxtamembrane area to the entire cytoplasmic area at GV stage. Thus, the full scope of mitochondrial dynamics during the maturation of human oocytes remains obscure.

Microtubules and microfilaments play critical roles in spindle formation, chromosomal segregation, and subcellular trafficking of various organelles including oocyte mitochondria [1, 2]. It has been postulated that mitochondrial movement during oocyte maturation is controlled by microtubules [9, 15, 23–25]. In contrast, actin filaments have been shown to play important roles in spindle positioning and cytokinesis [26], mitochondrial clustering in mouse oocytes [27] and their movement in pig oocytes [28].

Although analysis of fixed cells has contributed significantly to our understanding of characteristics of mammalian oocytes, dynamic aspects of mitochondrial distribution and its relation with the cytoskeleton in maturing human oocytes remain largely unknown. Time-lapse imaging of live oocytes permits detailed analysis of the role of mitochondrial dynamics in the maturation of human oocytes. The present work describes the dynamics of mitochondria and their relationship with the cytoskeleton in human oocytes during meiotic maturation.

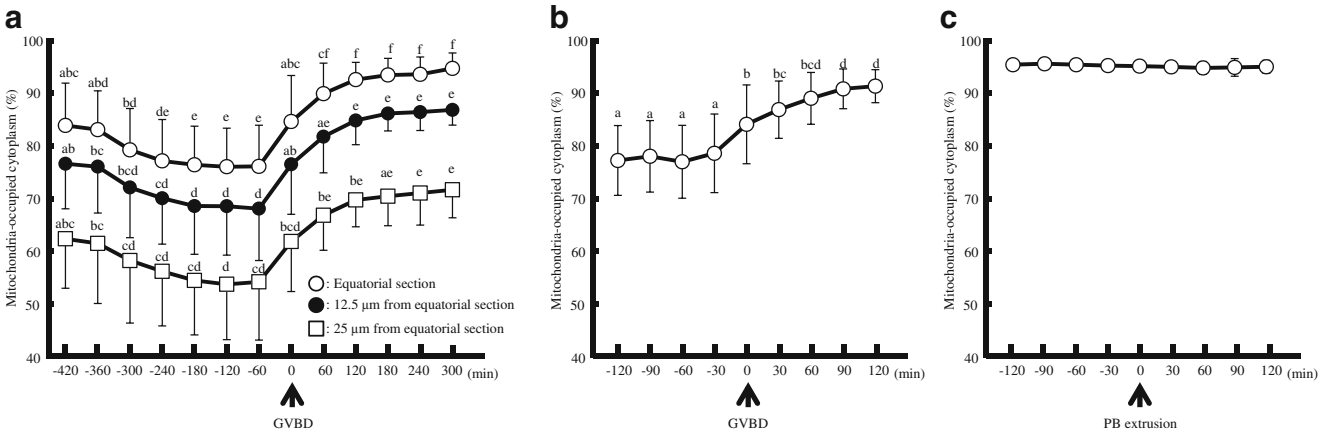

Fig. 2 Time-dependent changes of the mitochondria-occupied area (percentage of total) of the cytoplasm in maturing oocytes. **a** Time-dependent changes of the mitochondria-occupied area −420 min before and 300 min after GVBD obtained from 16 oocytes. The occurrence of GVBD was defined as the 0–min (*A* and *B*). **b** Time-dependent changes of the mitochondria-occupied area −120 min before and 120 min after GVBD obtained from 27 oocytes. **c** Time-dependent changes of the mitochondria-occupied area between −120 min before and 120 min after polar body (PB) extrusion obtained from 27 oocytes. The occurrence of PB extrusion was defined as the 0 min. Data points were compared by Fisher's PLSD test following ANOVA. *a–c*, $p < 0.01$. Characteristics of oocytes examined in live imaging study were shown in Table 1. Data and donor age were shown mean ± SD

Materials and methods

Oocyte collection

Donor patients were treated with controlled ovarian stimulation according to their medical history as previously described [29]. For gonadotropin-releasing hormone (GnRH) agonist cycles, patients received oral contraceptive pills (OC, 1 mg Norethisterone and 0.05 mg Mestranol, Aska Pharmaceutical, Co., Ltd., Tokyo, Japan) on day 14 of the previous cycle and continued for 10 days and GnRH agonist (600 μg/day, Suprecur® nasal solution 0.15 %; Mochida Pharmaceutical; Tokyo, Japan) on day 21 of the previous cycle until ovulation induction. On day 3 of the cycle, they received recombinant FSH (Gonal F, Merck Serono Co., Ltd., Tokyo, Japan) ranging from 150 to 300 IU for 4 days followed by HMG (Ferring Pharmaceuticals Co., Ltd., Tokyo, Japan) ranging from 150 to 450 IU administration until ovulation induction. For GnRH antagonist cycles, GnRH antagonist (2.5 mg, Ganirelix Acetate, MSD, Tokyo, Japan) was administered daily after leading follicles reached 13–14 mm in diameter. Ovulation induction was performed by human chorionic gonadotropin (hCG) administration when at least leading follicles reached 18 mm in diameter. Transvaginal follicle aspiration was carried out 36 h after hCG injection. Immature human oocytes were donated for research at the time of insemination by intra-cytoplasmic sperm injection (ICSI) 42 h after administration of hCG, and stained with a fluorescent dye followed by live cell imaging or fixed for ultrastructural analysis. Mature oocytes were obtained after additional culture of donated immature oocytes. Oocytes were collected between June 2013 and February 2016.

Ethical approval

This study was approved by the local ethics Institutional Review Board of IVF Namba Clinic and by the Japan Society of Obstetrics and Gynecology (Registry No. 144 and 146). All donor patients received a full explanation of the experiments and provided the signed informed consent. In Japan, the donation of oocytes which are mature 42 h after hCG injection is not generally admitted because of ethical reasons. Thus, in this study, we used oocytes with delayed cell cycle.

Live cell imaging

A total of 130 GV and 58 GVBD oocytes were donated for the live cell imaging studies at the time of insemination by ICSI 42 h after administration of hCG. Mitochondrial staining was carried out by incubating oocytes without cumulus cells in TCM199 Hank's salt solution containing 0.5 μM MitoTracker Orange CM-H2TMRos (M-7511, Life Technology, Carlsbad, CA, USA) at 37 °C for 0.5 h. Immediately, the cells were cultured in 5 μL IVM medium (82214010; Origio Japan, Kanagawa, Japan) [30] on a glass-bottom dish (P35G-0-14-C; Mat-Tek, Bratislava, Slovakia) [29].

Twenty images in the z-axis of live cell images were captured during oocyte maturation every 15 min for 40 h using a spinning disc confocal laser microscope equipped with an environmental chamber (excitation 561 nm, emission

Table 1 Characteristics of oocytes donated for live imaging

Oocyte cultured	Numbers of			Oocyte diameter (μm)	Donor age (year)	Numbers of stimulation cycles with		Causes of infertility				
	Patients	Cycles	Oocytes			Agonist	Antagonist	Endometriosis	Myoma	Oviduct PCO	Thyroid dysfunction	Unknown
Between −420 and 300 min of GVBD[a]	15	15	16	112.1 ± 4.3	38.8 ± 3.6	5	11	0	4	7	1 7	3
Between −120 and 120 min of GVBD[b]	23	23	27	111.1 ± 4.3	37.9 ± 4.4	10	17	1	6	13	1 10	6
Between −120 and 60 min of PB extrusion[c]	20	20	27	111.6 ± 4.7	37.8 ± 3.5	12	15	3	4	10	0 4	12
With colchcine Between −420 and 300 min of GVBD[d]	10	10	11	112.9 ± 3.4	38.8 ± 3.5	3	8	1	0	3	0 1	7
With cytochalasin B Between −420 and 300 min of GVBD[e]	9	9	9	113.7 ± 2.1	38.0 ± 5.6	3	8	1	2	3	1 1	3

[a–c] Live cell imaging of oocytes in Figs. 1 and 2

[a, d, e] Live cell imaging of oocytes cultured with an inhibitor for tubulin or actin filament in Fig. 5. Oocyte diameter and donor age were shown mean ± SD

BP617/73, CellVoyager CV1000; Yokogawa Electronic, Tokyo, Japan) [29]. This system enabled extended imaging studies of live cells remarkably free of fluorescence photobleaching [31]. Oocytes that were cultured in the absence of inhibitors and reached MII stage were used for the control experiment. Mitochondrial dynamics was analysed in the presence of either 20 μg/mL colchicine (039-03851, Wako, Osaka, Japan) or 0.1 μg/mL cytochalasin B (C6762, Sigma-Aldrich) to investigate the possible involvement of the cytoskeleton in the intracellular trafficking of mitochondria during meiotic maturation. Oocytes that required longer than 2 h for meiotic resumption after imaging were included in the analysis of mitochondrial localization.

Electron microscopy

To assess the mitochondrial structure and distribution in oocytes, 43 oocytes at various maturation stages (19 GV and 24 GVBD including 6 mature oocytes) were fixed in 1 % glutaraldehyde in a phosphate buffer (pH 7.4) at 4 °C for 24 h as previously described [32]. The specimens were washed in the same buffer overnight and post-fixed in 1 % osmium tetroxide at 4 °C for 2 h. After dehydration using increasing concentrations of ethanol, the samples were immersed twice in n-butyl glycidyl ether at 25 °C for 10 min. Samples thus treated were washed in a mixture of 50 % n-butyl glycidyl ether and 50 % Epon 812 resin (TABB Laboratories, Berkshire, UK) overnight and then embedded in Epon 812 resin. Ultra-thin sections were stained with uranyl acetate for 10 min and Reynold's lead citrate for 10 min and then examined using transmission electron microscopy (TEM, JEM-1011; JEOL Datum, Tokyo, Japan).

Analysis of mitochondrial localization in cells

To assess changes in the intracellular localization of mitochondria, the mitochondria-occupied area in the equatorial plane of oocytes was measured using ImageJ (http://imagej.nih.gov/ij/). Using MitoTracker-stained oocytes, the ratio of the area of cytoplasm containing mitochondria was calculated using and expressed as a percentage of the total cytoplasmic area.

Analysis of area ratio of mitochondria in cytoplasm at peripheral and perinuclear regions

Area ratio of mitochondria in cytoplasm was estimated by calculating the surface ratio of mitochondria per surface area of the oocyte at peripheral and perinuclear regions (10×10 μm^2) of TEM images at ×15,000 magnification. Surface areas of each mitochondria, oocytes were calculated using Dipp–Image version 1.0.5 (DITECT corporation, Tokyo, Japan) according to the manufacturer's instructions.

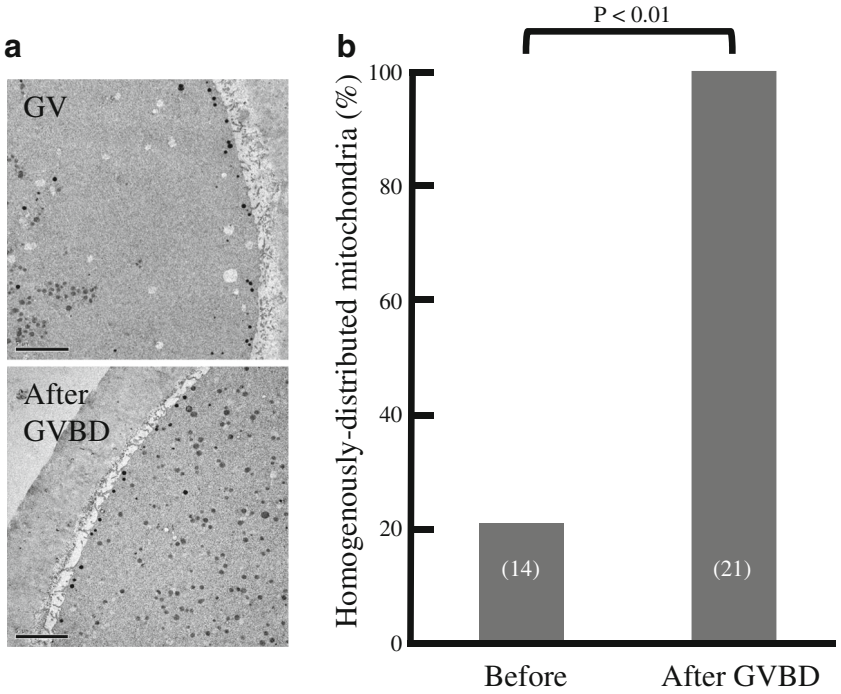

Fig. 3 Mitochondrial distribution during meiotic maturation of human oocytes. **a** TEM images of oocytes during meiotic maturation. No significant mitochondria were found in the juxtamembrane area of GV stage oocytes (*upper image*). Most mitochondria displayed a cluster-like distribution. Mitochondria were distributed homogenously in the cytoplasm after GVBD (*lower image*). **b** Proportions of oocytes with homogenously distributed mitochondria before and after GVBD were analysed morphometrically using TEM images. The numbers of examined oocytes are shown in *parenthesis*. Data were compared by student's *t* test. Original magnification ×5,000. *Scale bar* = 5 μm. Characteristics of oocytes used in this study were shown in Table 2. Donor age was shown mean ± SD

Statistical analysis

Differences between two groups were analysed using unpaired Student's *t* tests. When more than two groups were compared, analysis of variance (ANOVA) followed by Fisher's protected least significant difference (PLSD) testing was used. Data are represented as the mean ± SD. Statistical analysis was performed using StatView version 5 (SAS Institute Inc., Cary, NC, USA), and $p < 0.01$ was considered significant.

Results

As nuclear maturation proceeds, the distribution of mitochondria markedly changed (Figs. 1 and 2). The cytoplasmic area at equatorial section occupied by mitochondria decreased from 83 to 77 % between 360 and 240 min before GVBD ($n = 16$; Fig. 2a, Table 1). A similar pattern was indicated in other sections. Subsequently, the mitochondria-occupied area markedly increased to 85 % around the time of GVBD ($n = 27$; Fig. 2b). On the other hand, there was no significant change before and after polar body (PB) extrusion ($n = 27$; Fig. 2c). Analysis of TEM images revealed that most mitochondria localized centrally in the cytoplasm of oocytes before GVBD; no significant amount of mitochondria was found to localize in their subcortical areas (Fig. 3, Table 2). However, they localized homogenously in the entire area of cytoplasm after GVBD. The area ratio of mitochondria in cytoplasm at peripheral region of GV oocytes (0.98 %, Fig. 4a) was significantly lower ($p < 0.01$) than those of GVBD (3.86 %) and mature oocytes (4 %). The area ratio of mitochondria in cytoplasm at perinuclear region of GV oocytes (7.71 %, Fig. 4b) was significantly higher ($p < 0.01$) than those of GVBD (4.18 %) and mature oocytes (4.25 %). Moreover, the area ratio of mitochondria in cytoplasm at peripheral region (0.98 %, Fig. 4c) was significantly lower ($p < 0.01$) than that at perinuclear region of GV oocytes (7.71 %), but no differences in GVBD and mature oocytes. The data obtained using confocal imaging was consistent with TEM data. Mitochondria surrounding or co-localizing chromosomes or spindle were not observed (Fig. 1).

To test the possible involvement of the cytoskeleton in the subcellular localization of mitochondria, oocytes were cultured in the presence or absence of colchicine or cytochalasin B, inhibitors for tubulin and actin filament, respectively. In the absence of inhibitors, about 93 % of oocytes underwent GVBD, while the presence of inhibitors decreased this rate to 56 % (colchicine) and 59 %

Table 2 Characteristics of oocytes donated for TEM

Oocyte fixed at	Numbers of			Donor age (year)	Numbers of stimulation cycles with		Causes of infertility					
	Patients	Cycles	Oocytes		Agonist	Antagonist	Endometriosis	Myoma	Oviduct	PCO	Thyroid dysfunction	Uterus	Unknown
GV[a]	10	10	14	36.2 ± 2.4	10	4	0	0	7	0	1	0	6
GVBD[b]	15	15	21	37.9 ± 3	14	7	1	0	4	0	2	1	14
GV[c]	3	3	3	35.6 ± 3.2	1	2	0	0	1	0	0	0	2
GVBD[d]	3	3	3	38.2 ± 3.2	2	1	0	0	1	0	0	0	2
MII[e]	3	3	3	36 ± 5.3	2	1	0	0	0	1	0	0	2
GVBD[f]	9	9	15	37.2 ± 3	11	4	0	0	3	0	2	0	11
Mature[g]	6	6	6	40 ± 1.4	3	3	1	0	1	0	0	1	3
Colchicine -treated GV[h]	2	2	5[i]	32.8 ± 0.3	5	0	0	0	0	1	0	0	4
Cytochalasin B -treated GVBD[j]	3	3	3[i]	44.5 ± 2.7	0	3	1	0	0	0	0	0	2

[a, b] Analysis of mitochondrial localization by TEM in Fig. 3

[c–e] Analysis of are ratio of mitochondria by TEM in Fig. 4

[a, f, g, h, j] Analysis of mitochondrial clustering by TEM in Fig. 6

[i] Oocytes were fixed after live imaging. Donor age was shown mean ± SD

(cytochalasin B), respectively (Table 3). The maturation rate of the GV oocytes in the absence of inhibitors was almost 70 % while no oocytes matured in the presence of either inhibitor. Such changes in mitochondrial dynamics were affected significantly by the presence of the inhibitors (Fig. 5). In the presence of colchicine, the mitochondria-occupied area rapidly increased to 90 % of the cytoplasm at GV stage and remained unchanged during and after GVBD. In contrast, cytochalasin B rapidly decreased the mitochondria-occupied area of GV stage oocytes to 80 %. Although the mitochondria-occupied area also increased during GVBD in the presence of cytochalasin B ($p < 0.01$; −60 min, 75 % vs. 300 min, 87 %), it was fairly slow compared with the oocytes cultured in the absence of the inhibitors (Fig. 5).

Analysis using TEM revealed that mitochondria localized predominantly as a cluster-like structure in GV stage oocytes as shown previously [1, 2]. However, these clusters disappeared after GVBD and in colchicine-treated GV oocyte (Fig. 6).On the other hand, mitochondria remained at perinuclear region in cytochalsin B-treated oocytes after GVBD (Fig. 6a (10)).

Taken together, the clustered mitochondria localized predominantly in the extra-subcortical region of the cytoplasm at GV stage and occupied more than 80 % of the cytoplasmic area. This area decreased significantly and mitochondria localized more towards the perinuclear region at 5 to 6 h before GVBD. At GVBD, the mitochondria-occupied area rapidly increased to 90 % of the cytoplasmic area by some cytoskeleton-dependent mechanism(s). The ultrastructural analysis also showed similar results.

Discussion

The present work shows that the mitochondria-occupied cytoplasmic area in human oocytes markedly changed during their maturation.

Changes in mitochondrial distribution during maturation have been mapped in murine oocytes. Studies using mouse oocytes found that mitochondria formed aggregates around the nucleus of immature cells [9, 21, 22]. Mitochondria dispersed homogenously in the entire cytoplasm around GVBD and then they surrounded the MI spindle [22, 24]. Consistent with previous observation using fixed human oocytes [1, 2], the present work using confocal live imaging and TEM shows that the subcortical region of cell membranes of GV stage oocytes lacks mitochondria, however, it is filled with mitochondria following GVBD. The present work also shows that the mitochondrial accumulation of surrounding MI spindle was not appeared, thus, the pattern of mitochondrial distribution varies significantly depending on animal species. In addition, live cell imaging data revealed that mitochondria

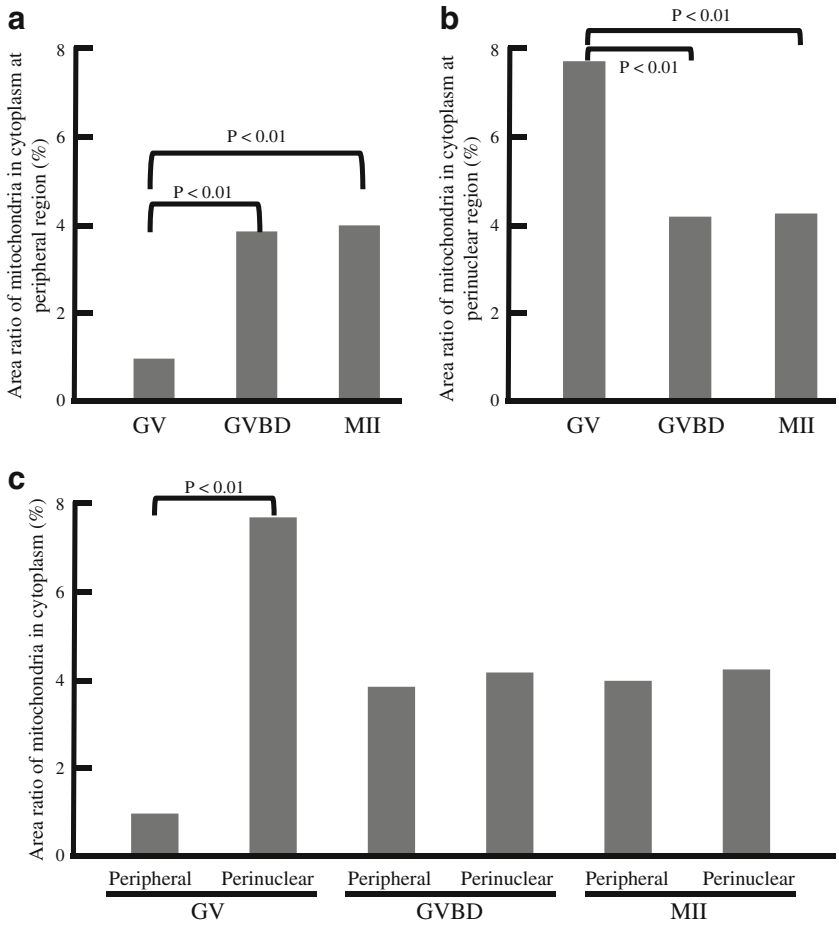

Fig. 4 The area ratio of mitochondria in cytoplasm at perinuclear and peripheral regions obtained from TEM (×15,000) images. The area ratio of mitochondria in cytoplasm at peripheral region (**a**) and perinuclear region (**b**) of GV, GVBD and mature (MII) oocytes. **c** The area ratio of mitochondria in cytoplasm at perinuclear and peripheral regions of GV, GVBD and MII oocytes. Data were compared by Fisher's PLSD test following ANOVA (**a** and **b**) and by student's *t* test (**c**). Characteristics of oocytes used in this study were shown in Table 2

localized at GV stage moved towards the perinuclear region at 5 to 6 h before GVBD. The transient decrease of mitochondria-occupied area before GVBD might reflect similar changes in mito-ring formation observed in mice oocyte [27].

Since mitochondria supply more than 90 % of cellular ATP [33], they play important roles in the progression of cell cycle [34]. During cell division, cells require additional ATP to enter mitosis from the G2 stage [35]. In fact, mitochondria accumulate at the perinuclear regions and spindles during meiotic maturation of oocytes [27]. The movement of mitochondria towards the perinuclear region might be important to locally increase the ATP supply to promote G2/M transition. In addition, mitochondrial ATP production has been shown to be required for maintaining a low intracellular Ca^{2+} and for sustaining sperm-triggered Ca^{2+} oscillations [18, 19]. Mitochondria in oocytes have been also shown to associate characteristically with smooth endoplasmic reticulum [1, 2].

Table 3 Meiotic maturation of human oocytes cultured with or without tubulin or actin filament polymerization inhibitor

	No. of examined	Oocyte stage at the start of imaging	Donor age	Stimulation		Proportion (%)	
				Agonist	Antagonist	GVBD	mature
Control	58	GV	37.9	27	31	93	66
	32	GVBD	40.5	12	20	–	72
+ Colchicine (20 μg/mL)	45	GV	37.1	18	27	56	0
	11	GVBD	37.0	6	5	–	0
+Cytochalasin B (0.1 μg/mL)	27	GV	38.5	4	23	59	0
	15	GVBD	38.5	0	15	–	0

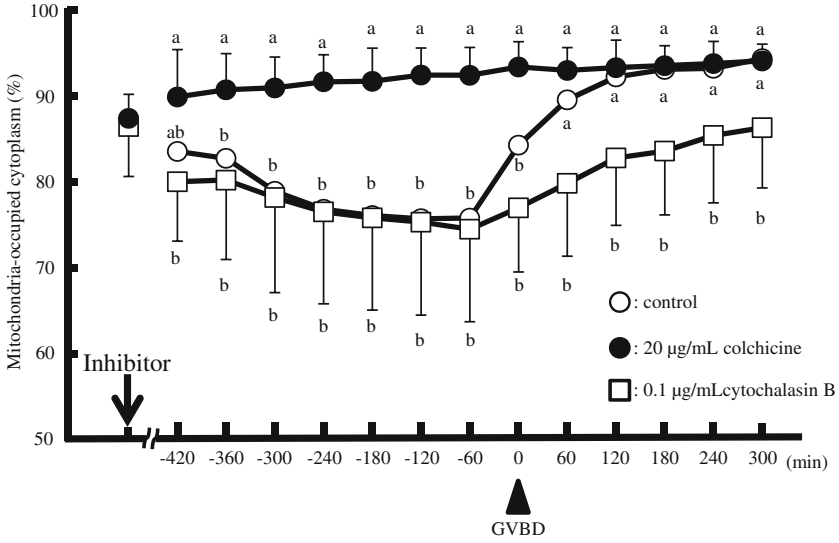

Fig. 5 Time-dependent changes of the mitochondria-occupied area (percentage of total) in oocytes in the absence (*open circles*) or presence of colchicine (20 μg/mL, *closed circles*) or cytochalasin B (0.1 μg/mL, *open squares*). Data were compared among experiments with and without inhibitors and analysed by Fisher's PLSD test following ANOVA (*a–b*, $p < 0.01$). The *arrow* and *arrowhead* indicate the time point when the inhibitors were added and the time of GVBD, respectively. Characteristics of oocytes used in this study were shown in Table 1

Recently, the distribution pattern of endoplasmic reticulum has been shown to change during meiotic maturation in human [36]. Because the penetration of sperm across the oocyte plasma membrane triggers Ca^{2+} oscillation, which are regulated by endoplasmic reticulum and/or mitochondria, the dynamic changes in mitochondrial localization observed in the present study might play critical roles in the process of fertilization and subsequent development.

a

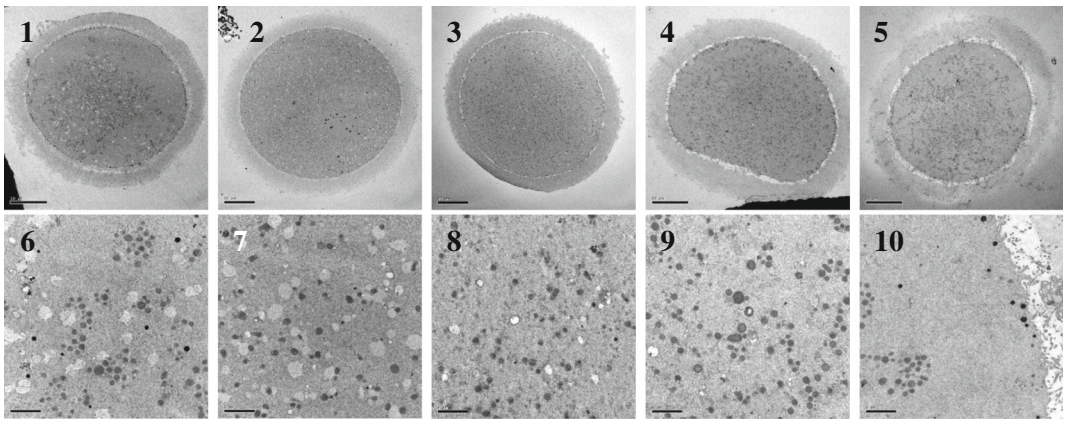

b Mitochondrial clustering during maturation (%)

	GV	GVBD	Mature	colchicine-treated GV	cytochalasin B-treated GVBD
No. of oocytes	14	15	6	5	3
Highly-clustered	64.3	0	0	20	0
Intermediate	21.4	33.3	16.7	80	66.7
Non-clustered	14.3	66.7	83.3	0	33.3

Fig. 6 TEM images of mitochondrial clusters during oocyte maturation. **a** TEM images of mitochondria before (*1*, *6*) and after (*2*, *3*, *7*, *8*) GVBD, Colchicine-treated GV oocyte (*4*, *9*) and cytochalasin B-treated GVBD oocyte (*5*, *10*). Mitochondria formed aggregates before GVBD in *panels 1* and *6* but the aggregates were not present in GVBD oocytes (*2*, *3*, *7*, *8*) and colchicine-treated GV oocyte (*4*, *9*). Mitochondrial clusters were observed in cytochalasin B-treated GVBD oocytes (*5*, *10*). **b** The amount of mitochondrial clusters was quantitated before and after GVBD using TEM images. Characteristics of oocytes used in this study were shown in Table 2. Original magnification in **a**: ×1,200 (*1* and *5*), ×1,000 (*2–4*), ×10,000 (*6–10*). *Scale bar* = 20 μm (*1–5*) and 2 μm (*6–10*)

Locomotion of mitochondria in oocytes during their maturation has been studied using mice [21, 27], pigs [15, 28] and human specimens [23]. Colchicine increased the mitochondria-occupied area in cytoplasm and inhibited their redistributions towards the perinuclear region around 6–7 h before GVBD, suggesting that microtubules played important roles both in the centripetal and centrifugal movements of mitochondria at the G2/M transition. In contrast, cytochalasin B rapidly decreased the mitochondria-occupied area and slightly inhibited the increase observed in control oocytes at the GVBD stage. This observation suggests that microfilaments also play important roles in the movement and localization of mitochondria close to the subcortical area of plasma membranes. In this context, microfilaments have been well documented to localize to subcortical areas along through plasma membranes and interact with the anchoring domain of the plus end of microtubules to form 3D network of the cytoskeleton. Since mitochondrial traffic in cells has been known to interact with kinesin and dynein to move along microtubules [37], it is not surprising that the mitochondrial movement and/or localization in human oocytes were affected differently by colchicine and cytochalasin B (Fig. 3). It has been shown that the pattern of mitochondrial distribution differed according to the meiotic competence [38]. Although the distribution pattern of oocytes which reached metaphase II was the same as obtained in live imaging study in the present study (data not shown). Further studies should be performed to assess the relationship with the pattern of mitochondrial distribution of immature oocytes and their meiotic competence.

Our observations suggest that both centripetal and centrifugal movements of mitochondria in maturing human oocytes occur along microtubules anchoring to microfilaments localized at the subcortical regions. Since cytochalasin B rapidly decreased the mitochondria-occupied cytoplasmic area, this inhibitor would have inhibited the anchoring to disturb the 3D network formed by microtubules and microfilaments at the subcortical regions. This notion is consistent with the present findings that the increase in the mitochondria-occupied area after GVBD was also affected by cytochalasin B. Since colchicine rapidly increased the mitochondria-occupied area and inhibited the following decrease observed with control GV stage oocytes, this inhibitor would have disrupted the 3-D structure of the anchoring domain of the minus end of microtubules close to the nucleus. In this study, we used surplus immature oocytes and cultured without surrounding cells to capture confocal images. As previously suggested [39], possible differences in the distribution of mitochondria and other organelles between mature and immature oocytes 42 h after hCG administration should be studied further experiments.

Various types of mitochondrial aggregation were observed with maturing oocytes from different animal species [5, 6, 15–17, 21]. Yu et al. [27] reported that mitochondrial clustering and dispersion occurred twice during meiotic maturation of mouse oocytes and suggested its relationship with cellular energy demand. The present work clearly shows that mitochondria in human oocytes formed aggregates at the GV stage but distributed homogenously in the whole area of cytoplasm at the time of GVBD.

The critical role of the redistribution of mitochondria in human oocytes should be studied further with respect to the change in the site(s) and properties of energy-dependent metabolism required for cellular maturation. The interaction of microtubules and microfilaments at the subcortical region of human oocytes also requires further studies.

Acknowledgments We would like to thank Editage (www.editage.jp) for the English language editing.

Funding Part of this work was supported by a grant from IVF Namba Clinic to S.H.

Author's roles Y.T., S.H., and T.Y. were involved in the literature review, experimental design, data acquisition, interpretation, and analysis and manuscript preparation. H.G., M.Y., A.A., and H.M. performed the TEM. K.I., Y.N., and Y.M. prepared the oocytes. H.M., M.I., and N.S. were involved in the manuscript preparation.

Compliance with ethical standards

Conflict of interest None declared.

References

1. Motta PM, Nottola SA, Familiari G, Makabe S, Stallone T, Macchiarelli G. Morphodynamics of the follicular-luteal complex during early ovarian development and reproductive life. Int Rev Cytol. 2003;223:177–288.
2. Sathananthan AH. Ultrastructural changes during meiotic maturation in mammalian oocytes: unique aspects of the human oocyte. Microsc Res Tech. 1994;27:145–64.
3. Krisher RL, Bavister BD. Responses of oocytes and embryos to the culture environment. Theriogenology. 1998;59:103–14.
4. Van Blerkom J, Davis P, Lee J. ATP content of human oocytes and developmental potential and outcome after in-vitro fertilization and embryo transfer. Hum Reprod. 1995;10:415–24.
5. Van Blerkom J. Mitochondria in human oogenesis and preimplantation embryogenesis: engines of metabolism, ionic regulation and developmental competence. Reproduction. 2004;128:269–80.
6. Stojkovic M, Machado SA, Stojkovic P, Zakhartchenko V, Hutzler P, Goncalves PB, et al. Mitochondrial distribution and adenosine triphosphate content of bovine oocytes before and after in vitro maturation: correlation with morphological criteria and developmental capacity after in vitro fertilization and culture. Biol Reprod. 2001;64:904–9.
7. Van Blerkom J. Mitochondrial function in the human oocyte and embryo and their role in developmental competence. Mitochondrion. 2011;11:797–813.
8. Dalton CM, Szabadkai G, Carroll J. Measurement of ATP in single oocytes: impact of maturation and cumulus cells on levels and consumption. J Cell Physiol. 2014;229:353–61.

9. Van Blerkom J. Microtubule mediation of cytoplasmic and nuclear maturation during the early stages of resumed meiosis in cultured mouse oocytes. Proc Natl Acad Sci U S A. 1991;88:5031–5.
10. Nagai S, Mabuchi T, Hirata S, Shoda T, Kasai T, Yokota S, et al. Correlation of abnormal mitochondrial distribution in mouse oocytes with reduced developmental competence. Tohoku J Exp Med. 2006;210:137–44.
11. Eichenlaub-Ritter U, Wieczorek M, Lüke S, Seidel T. Age related changes in mitochondrial function and new approaches to study redox regulation in mammalian oocytes in response to age or maturation conditions. Mitochondrion. 2011;11:783–96.
12. Barnett DK, Kimura J, Bavister BD. Translocation of active mitochondria during hamster preimplantation embryo development studied by confocal laser scanning microscopy. Dev Dyn. 1996;205:64–72.
13. Van Blerkom J, Davis P, Alexander S. Differential mitochondrial distribution in human pronuclear embryos leads to disproportionate inheritance between blastomeres: Relationship to microtubular organization, ATP content and competence. Hum Reprod. 2000;15:2621–33.
14. Van Blerkom J, Davis P, Mathwig V, Alexander S. Domains of high-polarized and low-polarized mitochondria may occur in mouse and human oocytes and early embryos. Hum Reprod. 2002;17:393–406.
15. Sun QY, Wu GM, Lai L, Park KW, Cabot R, Cheong HT, et al. Translocation of active mitochondria during pig oocyte maturation, fertilization and early embryo development in vitro. Reproduction. 2001;122:155–63.
16. Wilding M, Dale B, Marino M, di Matteo L, Alviggi C, Pisaturo ML, et al. Mitochondrial aggregation patterns and activity in human oocytes and preimplantation embryos. Hum Reprod. 2001;16:909–17.
17. Zhang YZ, Ouyang YC, Hou Y, Schatten H, Chen DY, Sun QY. Mitochondrial behavior during oogenesis in zebrafish: a confocal microscopy analysis. Develop Growth Differ. 2008;50:189–201.
18. Dumollard R, Marangos P, Fitzharris G, Swann K, Duchen M, Carroll J. Sperm-triggered [Ca^{2+}] oscillations and Ca^{2+} homeostasis in the mouse egg have an absolute requirement for mitochondrial ATP production. Development. 2004;131:3057–67.
19. Dumollard R, Carroll J, Duchen MR, Campbell K, Swann K. Mitochondrial function and redox state in mammalian embryos. Semin Cell Dev Biol. 2009;20:346–53.
20. Bianchi S, Macchiarelli G, Micara G, Linari A, Boninsegna C, Aragona C, et al. Ultrastructural markers of quality are impaired in human metaphase II aged oocytes: a comparison between reproductive and in vitro aging. J Assist Reprod Genet. 2015;32:1343–58.
21. Van Blerkom J, Runner MN. Mitochondrial reorganization during resumption of arrested meiosis in the mouse oocyte. Am J Anat. 1984;171:335–55.
22. Dumollard R, Duchen M, Sardet C. Calcium signals and mitochondria at fertilisation. Semin Cell Dev Biol. 2006;17:314–23.
23. Liu S, Li Y, Feng HL, Yan JH, Li M, Ma SY, et al. Dynamic modulation of cytoskeleton during in vitro maturation in human oocytes. Am J Obstet Gynecol. 2010;203:e1–7.
24. Heggeness MH, Simon M, Singer SJ. Association of mitochondria with microtubules in cultured cells. Proc Natl Acad Sci U S A. 1978;75:3863–6.
25. Nangaku M, Sato-Yoshitake R, Okada Y, Noda Y, Takemura R, Yamazaki H, et al. KIF1B, a novel microtubule plus end-directed monomeric motor protein for transport of mitochondria. Cell. 1994;79:1209–20.
26. Azoury J, Verlhac MH, Dumont J. Actin filaments: key players in the control of asymmetric divisions in mouse oocytes. Biol Cell. 2009;101:69–76.
27. Yu Y, Dumollard R, Rossbach A, Lai FA, Swann K. Redistribution of mitochondria leads to bursts of ATP production during spontaneous mouse oocyte maturation. J Cell Physiol. 2010;224:672–80.
28. Yamochi T, Hashimoto S, Amo A, Goto H, Yamanaka M, Inoue M, et al. Mitochondrial dynamics and their intracellular traffic in porcine oocytes. Zygote. 2016. doi:10.1017/S0967199415000489.
29. Hashimoto S, Nakano T, Yamagata K, Inoue M, Morimoto Y, Nakaoka Y. Multinucleation per se is not always sufficient as a marker of abnormality to decide against transferring human embryos. Fertil Steril. 2016. doi:10.1016/j.fertnstert.2016.03.025.
30. Hashimoto S, Fukuda A, Murata Y, Kikkawa M, Oku H, Kanaya H, et al. Effect of aspiration vacuum on the developmental competence of immature human oocytes retrieved using a 20-gauge needle. Reprod Biomed Online. 2007;14:444–9.
31. Wang E, Babbey M, Dunn KW. Performance comparison between the high-speed Yokogawa spinning disc confocal system and single-point scanning confocal systems. J Microscopy. 2005;218:148–59.
32. Hashimoto S, Suzuki N, Yamanaka M, Hosoi Y, Ishizuka B, Morimoto Y. Effects of vitrification solutions and equilibration times on the morphology of cynomolgus ovarian tissues. Reprod Biomed Online. 2010;21:501–9.
33. Hatefi Y. The mitochondrial electron transport and oxidative phosphorylation system. Annu Rev Biochem. 1985;54:1015–69.
34. McBride HM, Neuspiel M, Wasiak S. Mitochondria: more than just a powerhouse. Curr Biol. 2006;16:R551–60.
35. Sweet S, Singh G. Changes in mitochondrial mass, membrane potential, and cellular adenosine triphosphate content during the cell cycle of human leukemic (HL-60) cells. J Cell Physiol. 1999;180:91–6.
36. De Santis L, Gandolfi F, Pennarossa G, Maffei S, Gismano E, Intra G, et al. Expression and intracytoplasmic distribution of staufen and calreticulin in maturing human oocytes. J Assist Reprod Genet. 2015;32:645–52.
37. Hirokawa N, Niwa S, Tanaka Y. Molecular motors in neurons: transport mechanisms and roles in brain function, development, and disease. Neuron. 2010;68:610–38.
38. Sánchez F, Romero S, De Vos M, Verheyen G, Smitz J. Human cumulus-enclosed germinal vesicle oocytes from early antral follicles reveal heterogeneous cellular and molecular features associated with in vitro maturation capacity. Hum Reprod. 2015;30:1396–409.
39. Coticchio G, Dal Canto M, Renzini MM, Guglielmo MG, Brambillasca F, Turchi D, et al. Oocyte maturation: gamete-somatic cells interactions, meiotic resumption, cytoskeletal dynamics and cytoplasmic reorganization. Hum Reprod Update. 2015;21:427–54.